

Leakage through Cracks in RC Shear Walls (Dynamic Behavior and Functional Integrity Tests on RC Shear Walls)

Hideto SAITO, Yasuo INADA

Shimizu Corporation, Tokyo, Japan

Akenori SHIBATA

Tohoku University, Sendai, Japan

Hideo YOKOSAWA

Nuclear Power Engineering Center, Tokyo, Japan

1 INTRODUCTION

The negative pressure inside of the building of BWR and at the annulus zone of PWR should be maintained under control even in the case that S1 design earthquake occurs after LOCA. "Leakage through cracks in reinforced concrete shear wall" is one of the important problems when considering the air-tightness of these structures after the earthquake.

In order to obtain the methods for estimating the leakage, two types of model tests were carried out as follows:

1) Basic test: twenty specimens were tested in order to investigate the air flow rate through a single crack at different crack width and under various differential pressure, approximately 20~1000mmAq.

2) Application test: four flat-plate specimens were also tested in order to investigate the air flow rate through multiple residual shear cracks at different stress intensities and under various differential pressure, approximately 20, 100, and 200mmAq.

In this paper, based on the tests and the analysis, the estimation formula for the air flow rate through a single crack and for the air flow rate through residual shear cracks are discussed.

2 TEST METHOD

2.1 Specimens

For the basic test, twenty specimens described in Table 1 and Fig.1 were tested. The specimens are dumb-bell shaped and had different combination of wall thickness, crack surface material and crossing re-bars. In Type A, a concrete crack was idealized as the smooth gap by two parallel plates. Three specimens, different in wall thickness (12, 24 and 60cm), were constructed. In Type B, 17 specimens were constructed so that a single crack should be formed in the concrete at the narrow part of the specimen. The walls were of four different thicknesses (12, 24, 60 and 120cm), three different types of aggregates (pea gravel, crushed stone and river gravel) were used. Three of Type B specimens had some re-bars crossing the crack.

For the application test, four flat-plate specimens described in Table 2 and Fig.2 were also tested. The variables of each specimen were the re-bar ratio (0.53% and 1.03%) and re-bar spacing (16cm and 25cm). The configuration and dimension were the same throughout all specimens and each specimen had three test portions.

SMIRT 11 Transactions Vol. H (August 1991) Tokyo, Japan, © 1991

2.2 Method of Loadings and Measurements

For the basic test, a tensile force was applied to each specimen so that a single crack should be formed at the middle of the specimen, and then the air flow rate was measured by setting the crack width and the differential pressure as follows:

Crack width: Target widths were 0.1, 0.15, and 0.2mm in Type A and in Type B with crossing re-bars, and approximately 0.25, 0.5, 0.75, and 1.0mm in Type B without crossing re-bar.

Differential pressure: Approximately 20, 100, 200, 500, and 1000mmAq were the target.

For the application test, each specimen was tested under reverse symmetric bending shear loading. Relative displacement and flexural deformation in the test portion were measured to obtain shear deformation. The loading cycle consisted of 6 repeat load levels, and each level had 5 cycles. The first level was up to crack initiation and the last level up to $\tau=35\text{kgf/cm}^2$. Here, τ refers to the mean shear stress defined as the load P divided by cross-sectional area of specimen. The flow rate, and the crack width and its length were measured at differential pressure of three levels (approximately 20, 100, 200mmAq), and then the cracked state was sketched. Width of the crack crossing horizontal re-bars was measured with stereoscopic microscopes (x50).

3 TEST RESULTS

For the basic test, the relationship between the various set factors and the flow rate are summarized as follows: According to the two-dimensional Poiseuille theory, the flow rate is proportional to the differential pressure and the cube of crack width, and is inversely proportional to the wall thickness. The test results in both Type A and Type B showed a similar tendency when the flow rate was not large. No difference in the flow rate was recognized regardless of the size of aggregates and with or without crossing re-bars.

For the application test, the cracked patterns were different from test portion to portion. However, since the cracked patterns on the rear surface were the same as the front for each portion, all cracks appeared to penetrate linearly. Proportional relationship between the flow rate and the differential pressure were observed when the flow rate was not large. Comparing the flow rate characteristics for each specimen, the flow rate tended to be smaller when the re-bar ratio was larger, and when the re-bar spacing was smaller while re-bar ratio was the same.

4 EVALUATION OF TEST RESULTS

4.1 Study for the Basic Test

The results of the basic test were studied using the two-dimensional Poiseuille theory expressed as

$$q = \frac{W^3 \times \Delta P \times L}{12 \times \mu \times T} \quad (1)$$

where q = flow rate from a single crack ($\ell/\text{min.}$), W = crack width (mm), L = crack length (cm), T = wall thickness (cm), ΔP = differential pressure (mmAq) and μ = viscosity of air ($3.098 \times 10^{-2} \text{mm}^2 \text{mmAqmin.}/\ell$, at 20°C and 1atm).

Fig.3 shows the calculated and measured values (for comparison) of Type A specimens, which focused on flow rate between smooth flat plates set parallel to one another. Measured values were nearly equal to the values calculated by means of the two-dimensional Poiseuille theory. This indicates that the testing method is justifiable.

The measured flow rate of Type B specimens, which focused on a single crack of

concrete, was generally smaller than the values calculated by means of the two-dimensional Poiseuille theory. The following formula was reached by multiplying formula (1) by constant C:

$$q = C \times \frac{W^3 \times \Delta P \times L}{12 \times \mu \times T} \quad (2)$$

Assuming that experimental data were distributed normally on a logarithmic scale, regression analysis was made and then a mean value of 0.249 for the constant C was determined. The C value for a boundary line of lower (95%) probability is 0.393. In calculation, experimental data for flow rate larger than approximately 10 ℓ/min. and for differential pressure larger than approximately 200mmAq should be excluded. The reason for this is that when flow rate and differential pressure are large, the proportionate relationship of flow rate and differential pressure, estimated with formula (2), cannot be satisfied. Fig.4 shows a comparison of the calculated and measured flow rates. From the figure, it can be seen that the measured flow rate can be thoroughly explained by formula (2).

As described above, since the large flow rate and the flow rate of cases with large differential pressure cannot be explained with the two-dimensional Poiseuille theory, formula (3) incorporating gas compressibility was applied:

$$f \times \frac{T}{W} = \frac{W^3 \times (P_1^2 - P_2^2)}{2 \times \rho_0 \times P_0 \times (q/L)^2} \quad (3)$$

where f = friction coefficient, P₀ = 1 atmospheric pressure (10332mmAq), P₁ = pressure at upstream end, P₂ = pressure at downstream end (P₂ = P₁ - ΔP) and ρ₀ = air density (3.412mm³mmAqcm(min./ℓ)², at 20°C and 1atm).

To determine flow rate q from formula (3), f was determined by applying the regression linear formula (4) to all Type B specimens:

$$f = a \times L / q + b \quad (4)$$

where a and b = constants.

Value a × L and b were determined by substituting the crack data for each specimen in formulas (5) and (6):

$$a \times L = C_a \times W^{n_a} + 12 \times \mu \times L / \rho_0 \quad (5)$$

$$b = C_b \times W^{n_b} \quad (6)$$

where C_a, C_b, n_a and n_b = constants.

The regression analysis was made with respect to each of these constants by substituting the experimental data. The following values were obtained.

$$C_a = 2.91, n_a = -0.572, C_b = 0.221, n_b = -0.870$$

The flow rate calculated by formula (3) and measured values are given in Fig.5. Calculated values correspond well with measured ones. Thus, it is possible to explain the flow rate using formula incorporating gas compressibility, even for cases with large flow rate and large differential pressure.

A comparison of calculated flow rate (determined by estimation formulas (2) and (3)) with measured flow rate is shown in Fig.6. Specimen LB-60-10 is used as a typical example. Estimation formula (2) corresponds well with test values within a range up to approximately 10 ℓ/min. of flow rate and about 200mmAq of differential pressure. Sufficient accuracy was obtained. Furthermore, it was verified that estimation formula (3) can thoroughly explain test results even when the flow rate and differential pressure are large.

4.2 Study for the Application Test

Based on the study for the basic test, the flow rate for multiple cracks in the application tests was calculated using the flow rate estimation formula (7) based on the formula (2):

$$Q = \sum_i \left\{ 0.249 \times \frac{W_i^3 \times \Delta P \times L_i}{12 \times \mu \times T} \right\} \quad (7)$$

where Q = flow rate per unit area (ℓ/min.), W_i = crack width (mm) and L_i =

crack length (cm).

Fig.7 compares the calculated and measured values for all specimens. Although the dispersion of the experimental data in the application test was slightly large (compared with Fig.3), the flow rate calculated using the crack data basically corresponded with the measured flow rate. Thus, the application test data was found to be reliable.

An estimation formula on the relationship between the actual maximum shear stress (hereafter referred to as shear stress) and the flow rate from residual shear cracks was developed.

Results of the basic and the application tests indicate that flow rate is inversely proportional to wall thickness and is proportional to differential pressure. Flow rate proportional to n_c -th power of shear stress can be expressed by formula (8):

$$Q = C_c \times \tau^{n_c} \times \Delta P / T \quad (8)$$

where τ = experienced maximum shear stress (kgf/cm²) and C_c = constant.

Fig.8 shows the shear stress vs flow rate relationship of each specimen. Regression lines for each specimen are also shown. The flow rate of specimens LA-0.5-160 and LA-1.0-250 is smaller than that of specimens LA-0.5-250A and LA-0.5-250B. When re-bar ratio is smaller, or when re-bar spacing is larger while re-bar ratio is the same, the flow rate tends to be larger. An estimation formula was prepared based on the measured results of specimens LA-0.5-250A and LA-0.5-250B, in which re-bar spacing was 25cm (the maximum spacing usually used in reactor buildings) and re-bar ratio was 0.5% (the minimum ratio usually used in reactor buildings).

Assuming that the experimental data of both specimens distribute normally on a logarithmic scale, regression analysis was made and then a mean value of $C_c = 1.52 \times 10^{-10}$ and $n_c = 6.09$ were obtained. As performed previously, data obtained after re-bar yielded was excluded. For a boundary line of lower probability (95%), the constant value C_c is 6.37×10^{-10} . Fig.9 shows the shear stress vs flow rate relationship and the obtained estimation formula. This formula thoroughly explains the test results; in addition, it is possible to estimate the flow rate safely by selecting a high value for the constant (C_c).

An estimation formula for the relationship between the actual maximum shear strain (hereafter referred to as shear strain) and the flow rate from residual shear cracks was developed.

As with the estimation formula using shear strain, flow rate proportional to n_d -th power of shear strain can be expressed by a formula (9):

$$Q = C_d \times \gamma^{n_d} \times \Delta P / T \quad (9)$$

where γ = experienced maximum shear strain and C_d = constant.

A mean value of $C_d = 2.24 \times 10^6$ and $n_d = 2.57$ were obtained by performing regression analysis on the assumption that experimental data of four specimens was distributed normally on a logarithmic scale. As performed previously, data obtained after re-bar yielded was excluded. For a boundary line of lower probability (95%), the constant value C_d is 1.18×10^7 . Fig.10 shows the shear strain vs flow rate relationship and the obtained estimation formula. This formula well explains the test results; in addition, it is possible to estimate the flow rate safely by selecting a high value for the constant (C_d).

5 CONCLUSIONS

Based on the basic test results, a simplified flow rate estimation formula for a single crack was obtained. The formula was applicable to small flow rate and differential pressure. Although slightly complicated, a flow rate estimation formula for a wider range was obtained. Based on the application test results, two types of flow rate estimation formulas for residual shear cracks could be developed: one using shear stress and another using shear strain. From the results of the experimental studies performed in this paper, it can be concluded

these formulas may be useful for estimating and evaluating the leakage through residual shear cracks of RC shear walls of reactor buildings.

6 ACKNOWLEDGMENT

These tests have been carried out under the auspices of the Nuclear Power Engineering Center (NUPEC), an organization of the Ministry of International Trade and Industry, as part of the Seismic Safety Analysis Code Improvement Test Project, since fiscal year 1986.

REFERENCE

Suzuki T., Takiguchi K. et al (1990). Leakage of Gas Through Cracked Concrete Wall, JOURNAL OF STRUCTURAL AND CONSTRUCTION ENGINEERING (Transactions of AIJ) No.416: pp.17-25.

Table 1 Specimens for the basic test

Type	specimen	wall thickness	crack surface material	crossing re-bar
Type A	LB-12-A	12 cm	chromium plate	—
	LB-24-A	24 cm	chromium plate	—
	LB-60-A	60 cm	chromium plate	—
Type B	LB-12-10 °	12 cm	pea gravel	—
	LB-12-10S	12 cm	pea gravel	2-D10
	LB-24-10	24 cm	pea gravel	—
	LB-60-10 °	60 cm	pea gravel	—
	LB-24-20 °	24 cm	crushed stone	—
	LB-60-20 °	60 cm	crushed stone	—
	LB-120-20 °	120 cm	crushed stone	—
	LB-120-20S	120 cm	crushed stone	4-D32
	LB-60-25 °	60 cm	river gravel	—
	LB-120-25 °	120 cm	river gravel	—
	LB-120-25S	120 cm	river gravel	4-D32

° Footnote: 2 specimens

Table 2 Specimens for the application test

Specimen	Wall thickness	Re-bar arrangement	Re-bar ratio
LA-0.5-250A	30 cm	2-D16 @25 cm	0.53 %
LA-0.5-250B	30 cm	2-D16 @25 cm	0.53 %
LA-0.5-160	30 cm	2-D13 @16 cm	0.53 %
LA-1.0-250	30 cm	2-D22 @25 cm	1.03 %

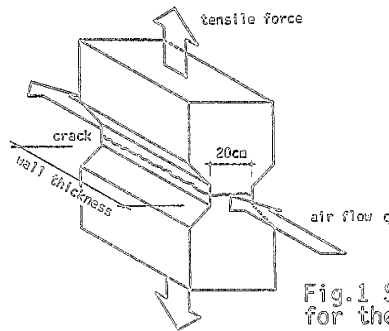


Fig.1 Specimens for the basic test

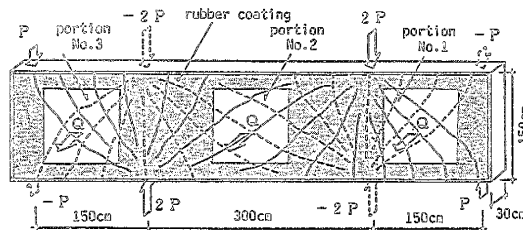


Fig.2 Specimens for the application test

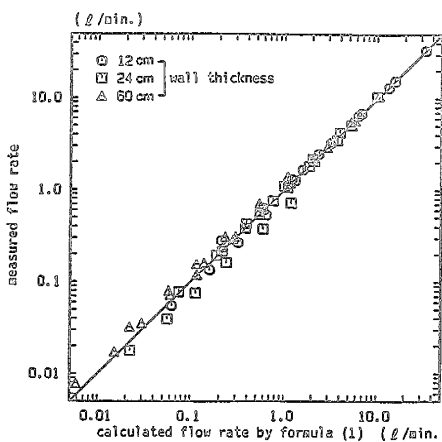


Fig.3 Comparison of calculated flow rate and measured flow rate (Type A)

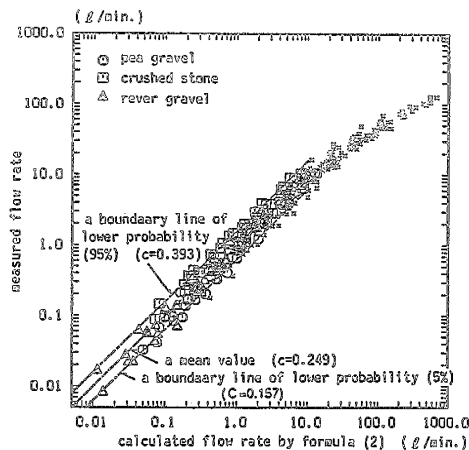


Fig.4 Comparison of calculated flow rate and measured flow rate (Type B)

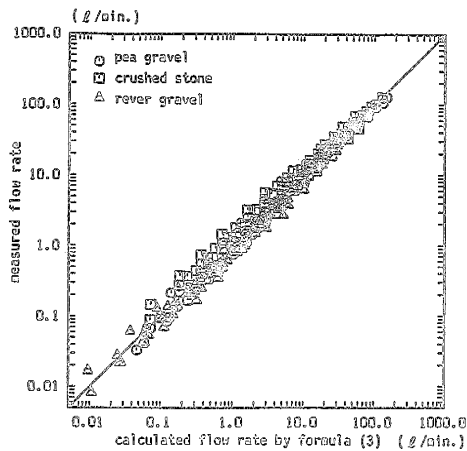


Fig.5 Comparison of calculated flow rate and measured flow rate (Type B)

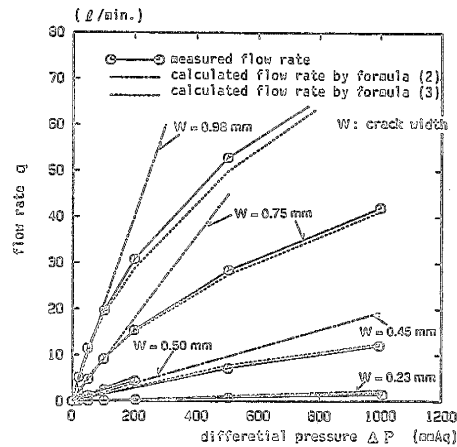


Fig.6 Comparison of calculated flow rate and measured flow rate (LB-60-10)

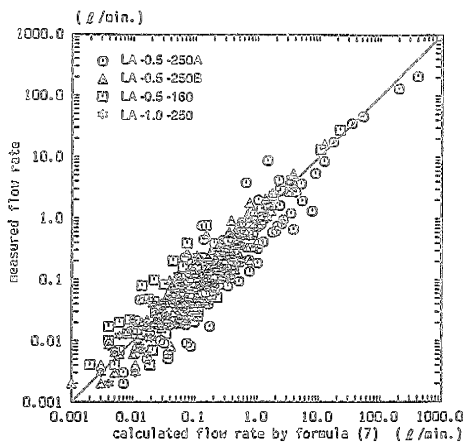


Fig.7 Comparison of calculated flow rate and measured flow rate

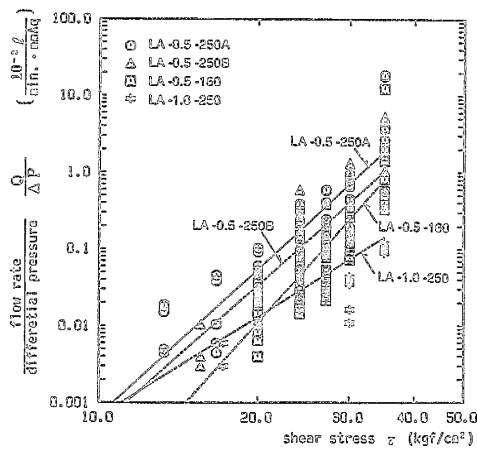


Fig.8 (flow rate / differential pressure) vs shear stress relationship

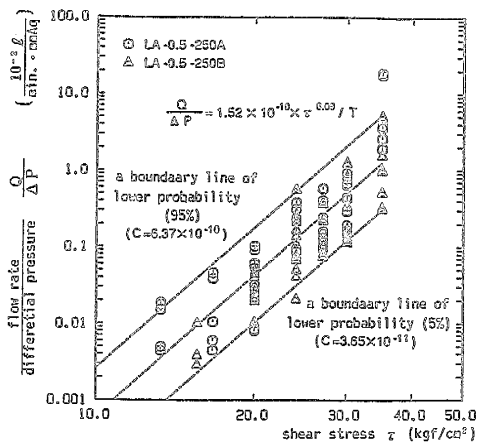


Fig.9 (flow rate / differential pressure) vs shear stress relationship

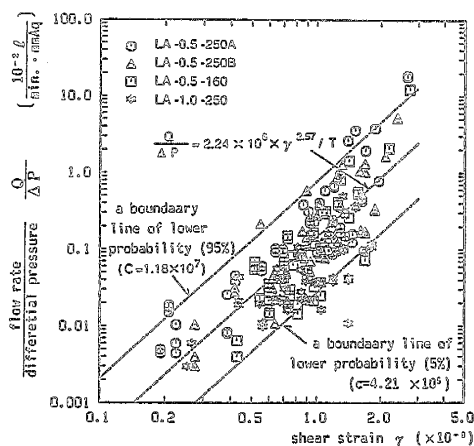


Fig.10 (flow rate / differential pressure) vs shear strain relationship